

Analysis of Performance Parameters of Amorphous Photovoltaic Modules under Different Environmental Conditions

A.A. Ghoneim^{1,*}; K.M. Kandil¹; A.Y. Al-Hasan²; M. S. Altouq¹; A.M. Al-asaad¹; L. M. Alshamari¹; A. A. Shamsaldeen¹

¹Applied Sciences Department, College of Technological Studies, Kuwait

Address: P.O. Box 42325, Shuwaikh 70654, Kuwait.

²Electronic Engineering Department, College of Technological Studies, Kuwait

Address: P.O. Box 42325, Shuwaikh 70654, Kuwait.

Supported by The Public Authority for Applied Education and Training (PAAET). The research team would like to express their sincere gratitude to PAAET for financial support of this work under the project No. (TS- 08- 02).

*Corresponding author.

Email: aa.ghoniem@paaet.edu.kw

Received 20 July, 2011; accepted 18 August, 2011.

Abstracts

The effects of temperature and radiation intensity on the performance parameters of amorphous hydrogenated silicon (a-Si:H) photovoltaic module have been investigated. An outdoor experimental setup is installed to carryout a series of I-V curve measurements under different irradiance and temperature conditions for the module. A numerical model which considers the effect of series and shunt resistances is developed to evaluate the different parameters of PV modules. Orthogonal distance regression (ODR) algorithm is adapted for fitting I-V measurements and extracting module parameters from I-V measurements. The values of module parameters, series resistance R_s , shunt resistance R_{sh} , diode ideality factor n and reverse saturation current I_0 determined from I-V measurements at different irradiation intensity and temperature range are in good agreement with the corresponding parameters obtained from the developed numerical model. The module parameters extracted from I-V measurements are employed to calculate the module performance parameters, i.e. open circuit voltage V_{oc} , fill factor FF and module efficiency η at different irradiation intensity and temperature range. Present results indicate that the module parameters have a significant effect on module performance. Also, the behavior of V_{oc} is

completely different at higher temperatures.

Key words: Amorphous module parameters; Ideality factor; Series resistance; Shunt resistance

Kandil, K.M., Al-Hasan, A.Y., Altouq, M. S., Al-asaad, A.M., Alshamari, L. M., Shamsaldeen, A. A., Ghoneim, A.A. (2011). Analysis of Performance Parameters of Amorphous Photovoltaic Modules under Different Environmental Conditions. *Energy Science and Technology*, 2(1), 43-50. Available from: URL: <http://www.cscanada.net/index.php/est/article/view/10.3968/j.est.1923847920110201.715> DOI: <http://dx.doi.org/10.3968/10.3968/j.est.1923847920110201.715>

INTRODUCTION

Photovoltaic technology clearly offers tremendous environmental benefits, requiring no fuel and producing no emissions or other waste beyond that inherent in the manufacturing process. The adaptation of thin film solar modules in many applications is growing in the last few decades due to their low cost and manufacturing technology. Amorphous silicon (a-Si) module is considered as one of the most promising technology for this area. So, the detailed outdoor behavior of these modules is required under different environmental conditions.

In a-Si module, the diffusion length of the charge carriers is much shorter than in crystalline silicon modules. So, in crystalline silicon modules, solar cell structure is based on the transport of minority carriers in the quasi neutral region of the pn junction, which is not the case for a-Si. Due to the very short diffusion length the photo-generated carriers would virtually all recombine in the doped layers of a-Si before reaching the depletion region of the pn junction. So, a different technique namely intrinsic layer is adapted to manufacture the a-Si solar cells. The photo-generated carriers move towards the doped layer (electrons toward the n-type and holes toward the p-type) and are collected by the electrodes. The

dominant transport mechanism of the photo-generated carriers is drift in the internal electric field and therefore a-Si solar cells are often called drift devices^[1].

The outdoor performance of a-Si modules under different solar irradiance and device temperature and or spectral irradiance is vital for selecting the proper solar module for certain location and specific application. Series and shunt resistances in solar cells are parasitic parameters, which significantly affect the illuminated I-V characteristics and cell efficiency. Series resistance, R_s , is mainly the sum of contact resistance on the front and back surfaces. So, the series resistance should be kept to a minimum for efficient conversion of solar energy. The shunt resistance, R_{sh} , represents a parallel high conductivity path across the p-n junction or the cell edges and decreases the efficiency of the cells by increasing the leakage current that lowers the maximum output power (P_m), the open voltage, V_{oc} and the fill factor, FF. Several methods are available in the literature for extracting the series and shunt resistances of a solar cell^[2-5] as well as related device parameters. Some of the methods involve measurement of illuminated I-V characteristics, some use dark conditions or utilize dark and illumination measurements. Other methods apply curve fitting method to some assumed functional relationship or employ integration procedures based on the computation of the area under the I-V curves or use linear regression. It is also possible to predict PV module performance under illumination through a several numerical or algebraic methods^[6-8]. Most of the above mentioned methods are based on single exponential model of solar cell and assume that the shunt resistance, R_{sh} , is infinite and presume that R_s is independent of the intensity of illumination which is not a correct assumptions especially for solar cells that have low R_{sh} as amorphous silicon and CIS modules.

For this reason, an improved five parameter model which considers the shunt resistance is developed to carry out the present work. The model can handle the different cell technologies namely amorphous crystalline and copper indium diselenide (CIS) thin-film modules. The five parameter model uses the data provided by the manufacturers and empirical correlation equations to predict the solar cell parameters at different operating conditions. Measurements of I-V characteristics are carried out in the photovoltaic facility installed at the roof of the main building in the College of Technological Studies, Kuwait. These measurements are carried out at different illumination intensity and temperature. Non linear curve fitting of experimental I-V data proposed by Burgers et al.^[9] is adapted to extract different solar modules parameters from I-V measurements. A comparison between solar modules parameters predicted from the developed numerical model and the corresponding parameters obtained from I-V measurements to validate the accuracy of the developed numerical model proposed

for this study. The module parameters extracted from I-V measurements are employed to calculate the module performance parameters, i.e. short circuit current (I_{sc}) open circuit voltage (V_{oc}), fill factor (FF) and module efficiency (η) at different irradiation intensity and temperature range.

1. THEORETICAL ANALYSIS

To choose an appropriate model for detailed simulation, several factors need to be considered. A PV cell is not a fixed voltage source, so the model should be able to predict the current and voltage over the entire operating voltage range. Another factor is whether the data required by the model is provided by the manufacturers or not. Another important consideration is whether the data needed to use an I-V model are readily available to the system designer. Models with a large number of parameters, although possibly more accurate, either requires access to generally unpublished and proprietary manufacturer's data, or else require prototype test data. The most detailed, consistent information commonly available is provided in brochures from commercial module manufacturers.

A five parameter photovoltaic model is adapted in this study to determine the module parameters. In the present work, the five parameter model is used to simulate the characteristic of thin film solar modules at different weather conditions. This model adds R_{sh} to the four-parameter model making it applicable to both crystalline and thin film PV solar cells.

The mathematical model describing the performance of the solar modules should accurately predict how solar module output would vary with ambient temperature and radiation conditions. Since the solar cell is a nonlinear power source, so the output current and voltage depend on the radiation level and temperature. There are different photovoltaic simulation programs developed for modeling the performance of the solar cell. In these models, the solar cell is treated as an equivalent circuit. Such models require a program to simultaneously determine the current-voltage (I-V) characteristics as well as the output of a PV module. The four parameters model is a widely used model for determining the characteristic curves of solar cells. The four-parameters appearing in the IV equation are the light current (I_L), the series resistance (R_s), and two theoretical diode characteristics. These parameters are not measurable quantities and are not generally included in manufactures catalog data. As a result, they must be determined from systems of I-V equations at various operating points; these points are taken from catalog data. The detailed analysis of the four-parameter PV model was introduced by Townsend^[6] and incorporated into TRNSYS^[10].

The four parameter model assumes that the slope of the I-V curve is flat at the short-circuit condition. This means that this model neglects R_{sh} because it is very

large compared with R_s for the crystalline silicon (C-Si) cell. However, this assumption is not generally valid for amorphous photovoltaic. So, the four parameters model accurately predicts the performance of single crystal and polycrystalline PV arrays. In the other hand, the four parameters model can not accurately predict the performance of thin film PV modules. The main deviation is around the maximum power point because a-Si solar cell does not have a good fill factor as the C-Si cell does. In order to explain the low fill factors measured, the shunt resistance, which are lower than that of C-Si cell should be taken into consideration. The five parameters model takes R_s into account. Adding this parameter makes the five-parameter model applicable to both crystalline and amorphous PV cells. In the present work, a five parameter model is developed to simulate the characteristics of amorphous module at different weather conditions. The electrical behavior of the five parameter model is usually described by the equation:

$$I = I_L - I_o \times \left\{ \exp\left(\frac{q}{nkT_c}(V + IR_s)\right) - 1 \right\} - \frac{V + IR_s}{R_{sh}} \quad (1)$$

Where I_L is the light current, I_o is the diode reverse saturation current. The diode current, I_D is the current flowing internally across the cell's semiconductor junction. All the internal dissipative electrical losses are lumped together into the series resistance, R_s . R_{sh} is the shunt resistance and as it approaches infinity, this arrangement becomes identical to the four-parameter model. Thus, all the equations employed in the five-parameter model reduce to those in the simpler four parameter scheme for very large values of R_{sh} . Equation (1) also includes ideality factor (n), electron charge (q), Boltzmann constant (k) and cell temperature (T_c). The five parameters from which the five parameter model obtains its name are: n , I_L , I_o , R_s , and R_{sh} . Amorphous silicon (a-Si) and copper indium diselenide (CIS) photovoltaic cells exhibit a pronounced slope at the short circuit point, therefore a finite shunt resistance exists. A numerical model is adapted to solve equation (1) to obtain the five parameters at different illumination intensity and operating temperatures. The magnitude of the IV slope at short-circuit is related inversely to the shunt resistance. As R_{sh} approaches infinity, this arrangement becomes identical to the four-parameter model. Thus, all the equations employed in the five-parameter model reduce to those in the simpler four parameter scheme for very large values of R_{sh} . An additional equation is needed to numerically solve I-V equation. The catalog value that is employed to get the additional equation is the temperature coefficient of open-circuit voltage (μ_{VOC}). The light current (I_L) parameter was observed to depend on the effective solar irradiance, the cell temperature (T_c), the short circuit current temperature coefficient (μ_{ISC}), and the air mass modifier. The equation for I_L is:

$$I_L = \frac{G}{G_{Ref}} \left[I_{L,Ref} + \mu_{ISC}(T_c - T_{C,Ref}) \right] \quad (2)$$

Subscript (Ref) refers to values at reference conditions.

1.1 FORTRAN Component for I-V Characteristics

Several computer-based Software such TRNSYS^[10] exist for estimating the performance of PV systems. An important distinction among models is whether the model performs simulations over frequent, usually hourly, intervals or whether a reduced set of calculations is done based on average behavior over a longer, usually monthly interval. The detailed models require extensive weather data; Typical Meteorological Year (TMY) data. Another major distinction is whether or not the model is limited to use on maximum power-tracked systems. None of the previous available models are able to model direct-coupled loads of arbitrary I-V shape. The method presented in this work uses long-term average weather data to estimate system output for direct-coupled loads of any I-V shape. The equations in the previous sections are implemented to develop a numerical model to determine the characteristics of a-Si:H module. FORTRAN code necessitates three different groups of information: a set of parameters, an array of input variables and an array of output variables. The parameters are characteristic values which are fixed through out the run. Inputs to the code are the time dependent variables such as irradiance and temperature. The output depends on the parameters needed to analyze the performance of PV modules. The iteration process begins with an initial guess of V as an input to the PV array component. The PV component calculates the corresponding current into the load component. The load component produces a new voltage serving as a second guess for PV array component. The successive substitution is continued until convergence is obtained.

1.2 Non Linear Curve Fitting of Experimental Data

To extract the PV module parameters a non linear curve fitting program IVFIT of experimental I-V data proposed by Burgers et al.^[9] is adapted for this study. Measurements of the I-V curves of solar modules are one of the most important means of obtaining information about PV modules. Straightforward least squares fitting of I-V curves leads to non accurate fit leading to a bad fit at the maximum power point and lower voltage values. The strongly varying slope makes it difficult to fit PV modules I-V curves with standard least square techniques. To deal with this problem, Burgers et al.^[9] propose using weighting functions to minimize the area between data and fit instead of least squares procedure. Voltage noise has a big influence on fitting due to the steep slope of an I-V curve for higher voltage values. So, Burgers et al.[9] have used Orthogonal Distance Regression (ODR) which

is a mathematical method for fitting measurements and in the meantime it allows for computing the I-V curve parameters. The goodness of fit, χ^2 , is used to judge whether the one- or two-diode models are suitable. The computer code adapted employs an iterative scheme such that the fitted current and not the measured current are used to calculate the effect of series resistance. The program accounts for noise in the current as well as in the voltage signal of the measured datasets. ODR algorithms process both the error signal of the current and of the voltage close to I_{sc} and V_{oc} . Noise levels determined from the IVFIT is checked such that the IV curve fit at STC proved to be as accurate as possible.

2. RESULTS AND DISCUSSIONS

A test facility is installed at the College of Technological Studies, Kuwait. This test facility is designed to measure the I-V characteristics of different types of PV modules at different radiation and temperature levels in Kuwait climate. The solar modules are mounted on the roof of the main building in the College of Technological Studies facing south at a tilt angle 31° which is equal to Kuwait latitude. The place of the solar modules is chosen such that a shadow will not be cast into the solar modules at any time during the test period.

The test method proposed for the measurement of the I-V characteristics of PV modules at different radiation and temperature levels requires the measurements of the following parameters: i) the global radiation on the solar module, ii) the I-V curve at different radiation levels and ii) the I-V curve at different temperature levels.

The intensity of the solar radiation incident on the module surface are measured and recorded by an Eppley Precision Spectral Pyranometers (PSP model) connected to the data acquisition system. Measurements are recorded for periods where variations in global radiation through

the measurement period do not exceed $\pm 20 \text{ W/m}^2$. The accuracy of the temperature measurements devices differ according to the purpose they are used for. The ambient air temperature should be measured within an accuracy of $\pm 0.1^\circ\text{C}$. A standard resistance thermometer detector (RTD-PT100) is used to monitor the surrounding ambient temperature to guarantee high accuracy for this critical temperature. It is to be noted that the RTD sensor of the ambient temperature is shaded from direct and diffuse solar radiation.

The Keithley Source Meter instrument is adapted to perform I-V characteristics of different solar cell modules. The Keithley Source Meter instrument combines a programmable power source with the measurement functions of a digital multimeter. The Keithley LabTracer software allows users to coordinate the measurement and sourcing voltage or current and collect voltage and/or current readings, as well as a timestamp for each measurement set. One can sweep voltage or current allowing collection of complete test sequences. Results can be exported to windows based programs like EXCEL spreadsheet for calculation, and analysis. During the module tests, the corresponding values of environmental parameters were recorded by Keithley 2700 data acquisition device. All of this information is saved to different data files in a personal computer. The obtained measured data files are treated first to eliminate erroneous points. The I-V curves are then plotted and a numerical technique is adapted to analyze the measured data and extract the different modules parameters. The I-V curves of amorphous silicon module were monitored for the period July 12, 2009 to July 28, 2010. The sourcemeter is used to sweep voltage through the solar modules and measure current to obtain the I-V curves.

Table 1 lists the manufacturer specifications of the module used in this study at reference conditions STC ($G_{Ref}=1000 \text{ W/m}^2$, $T_{C,Ref}=25^\circ\text{C}$).

Table 1
Modules Specifications

Parameter	P (W)	I_{sc} (A)	V_{oc} (V)	I_{mp} (A)	V_{mp} (V)	μ_{isc} (A/ $^\circ\text{C}$)	μ_{voc} (V/ $^\circ\text{C}$)	Area (m^2)	Junctions
a-Si:H	10	0.9	21.5	0.7	17.0	0.0003	-0.06	0.27	30

The I-V characteristics obtained from the present measurements agree well with the corresponding I-V characteristics provided by the module manufacturer. To check the reliability of the present numerical model, the measured I-V characteristics are compared to the corresponding characteristics obtained from the numerical model. The two predictions agree very well indicating the reliability of the adapted numerical model. It should be noted that both temperature coefficients of short circuit current (μ_{isc}) and open circuit voltage (μ_{voc}) are provided by the manufacturer of the module. All the data are repeated at different days and time for the same radiation

levels. So, the measured I-V points can be considered as the average points for the module during the test period. It was found that there is a linear increase in photo-generated current with increased photon flux as irradiance levels increase, resulting in an increase in current with increased irradiance. It is observed that there is a great variation in power produced from day to day due to the fluctuations in daily irradiation and other meteorological parameters such as temperature. The seasonal variation caused mainly by fewer sunshine hours in winter than in summer was also evident. The variation of power with voltage and the values of the maximum power produced

by the module are calculated for each radiation level. The maximum powers are calculated using the present developed model. These values are compared with the ones extracted from the non linear curve fitting of I-V data using the IV fit program^[9] and are found to be in good agreement. It was found that there is a significant increase in the module power with increased irradiance levels. It should be mentioned that the maximum power point is not always corresponding to solar noon which is 12:00. The reason for this behavior may be attributed to the fact that the amount of irradiance received by the module is at its maximum at solar noon. In the meantime there is a drop in open circuit voltage, V_{oc} , around solar noon, which may be attributed to the elevated temperatures at this time of the day. Also, it is observed that the voltage corresponding to maximum power point changes with radiation levels. The operating temperature of the PV module is one of the most important parameters affecting the solar module power output and its efficiency to convert sunlight into electricity. The output of the photovoltaic module decreases with increase of the cell temperature. In order to improve PV module maximum efficiency and output power, the module temperature must be reduced.

The I-V characteristics of amorphous module at different temperatures are studied. Different curves are measured around noon on different days at different module temperatures. The decrease in V_{oc} with increase in temperature was clearly illustrated by the present I-V measurements. Also, measurements indicate that V_{oc} is more temperature dependent than I_{sc} . The largest drop in V_{oc} to about 20°C increase in temperature is approximately 8.8% drop in V_{oc} which is not compensated for by the relatively small increase in current, (2.8% in I_{sc}), resulting in a reduction in P_{max} of 6.4%. If not taken into account, excessive temperatures coupled with variation in irradiation, can lead to under-designing of PV systems, which in turn may lead to system failure.

As stated before, the comparison between the results obtained from the numerical model and the experimental I-V data indicated the accuracy of the present measurements. So, the non linear curve fitting technique proposed by Burgers et al.^[9] is adapted to extract the PV module parameters from the experimental I-V data at different environmental conditions. The five parameters of the PV module are: I_L , I_o , R_s , R_{sh} and n . Results imply that I_L is directly proportional to irradiance intensity level. In the following we present a discussion for the effect of environmental conditions on the other four parameters of a-Si:H module.

The module parameters variation with radiation at ambient temperature, T_a , equal to 28°C is presented in Figure 1 and the corresponding performance parameters variation is presented in Figure 2. It is known that the two module parameters reverse saturation current (I_o) and ideality factor (n) are related to recombination processes in the pin layers of a-Si:H cells of the modules and to

the electronic inhomogeneity in the pin layers especially the absorber (i-layers) which is the critical layer of thin film solar cell where photo-generation and most of recombination occurs.

It is well known that in the low radiation intensity, most of the photo-generated carriers produced in the i-layer recombine due to the density of defect states and its reduced life time. So, as predicted from the figure, increasing irradiance intensity up to 800 W/m² results in decreasing I_o from 1.4×10^{-4} to 0.6×10^{-4} A and n from 3.9 to 2.9. This decrease continues until the module becomes more stable. Increasing intensity to higher levels (>800 W/m²), the number of recombination centers decreases and in this case the energy of the incident photons plus the energy produced due to recombination are enough to produce more defects at the back of the i-layer and near the i/n interface. This means that the dominant phenomena at high irradiance intensity is the recombination at the back interface between the i-layer and the doped n-layer which normally has high density of defect states^[11,12] not the recombination in the i-layer. As seen from the figure I_o and n at the end tend to saturate. The reason of this behavior may be attributed to the fact that the number of defects due to weak bonds or electronic inhomogeneity is self limited^[11,13].

On the other hand, the series resistance, R_s , exhibits a dramatic change with illumination intensity as presented in the figure. As stated by Hegedus^[11], R_s is a lumped series resistance which includes the sum of several contributions as spreading resistance through front or back electrodes, contact resistances with the window layers (ZnO/p or SnO₂/p) and through film resistance in the active absorber or emitter layers in the device. Also the collection grid contributes to the lumped resistance R_s . As presented by the figure, R_s starts to increase with increasing illumination (for low range) which is may be due to the contact resistance and barrier block in thin film solar cell which cause non-ohmic behavior at low irradiance. So, R_s is increased from approximately 6.5 to 12.3 Ω in this narrow range of irradiance. As the intensity is increased, R_s starts to decrease slowly in the medium range of irradiance then quickly in the high range (≥ 800 W/m²) which may be due to contact problems and defects at the back electrode near i/n interface. The shunt resistance, R_{sh} , represents any high conductivity paths through the solar cell or on the cell edges^[14]. These would be due to defects in and near the i-layer of a-Si:H solar cells and give rise to shunt currents. These shunt paths lead current away from the intended load and their effects are detrimental to the module performance especially at low irradiance level as shown in Figure 1 where its value starts with 325 Ω at low irradiance and decrease to 100 Ω at high irradiance. After prolonged exposure of thin film solar cells to light, the number of shunts may increase and consequently increases the effective shunt currents in the cell and decreases R_{sh} particularly at high irradiance level.

The behavior of module performance I_{sc} , V_{oc} , FF and η with irradiation intensity can be explain in view of the module parameters behavior as presented in Figure 2. Figure 2 indicates that I_{sc} increases linearly with increasing irradiance intensity except in the regions of low and high intensity where there is deviation from linearity may be attributed to the changes in Rs previously discussed in Figure 1. The effect of R_s on I_{sc} follows single exponential model of device at short circuit conditions where:

$$I_{sc} = \left(\frac{R_{sh}}{R_{sh} + R_s} \right) I_{ph} \quad (3)$$

The open circuit voltage V_{oc} decreases fastly at low irradiance from 21.6 V to 20.6 V and starts to decrease with a slow rate in the middle range to 20.3 V then starts to increase to 20.7 V close to high radiation intensity ($\geq 800 \text{ W/m}^2$). This behavior is opposite to the behavior of Rs but consistent with the changes in I_0 and n since V_{oc} is related to I_0 and n following the equation:

$$V_{oc} = \frac{E_g}{q} + \frac{nkT}{q} \ln \left[\frac{I_{ph}}{I_0} \right] \quad (4)$$

In equation (4) the changes of n in the 2nd term are nearly compensated by the changes of I_0 , so R_s should has the strongest effect on V_{oc} . The module efficiency η is expressed as :

$$\eta = \frac{FF I_{sc} V_{oc}}{GA} \quad (5)$$

where FF is the fill factor which is a measure of the junction quality and R_s . Equation (5) states that the behavior of η is considered as the combination behavior of the three parameters V_{oc} , I_{sc} and FF as shown from Figure 2.

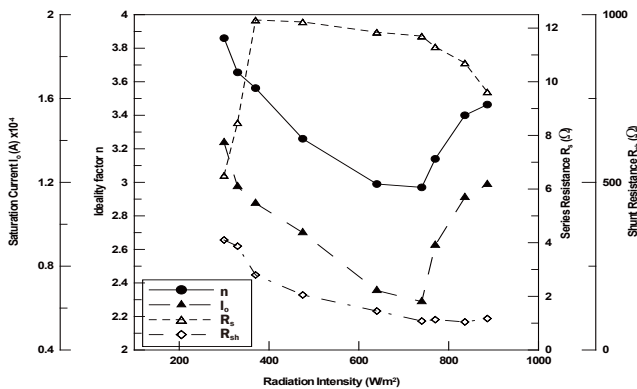


Figure 1
The Module Parameters Variation with Radiation Intensity at Ambient Temperature 28°C

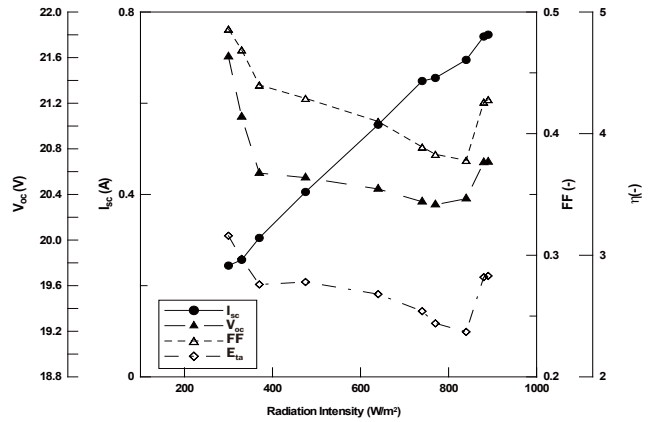


Figure 2
Variation of Module Performance Parameters with Radiation Intensity at Ambient Temperature 28°C

Figures 3 and 4 present the variations of module parameters and the corresponding module performance parameters at $T_a=38^\circ\text{C}$. The variation of module parameters with increasing irradiance is slightly changed from that previously presented at $T_a=28^\circ\text{C}$. This behavior of module parameters results in a strong change in the module performance as predicted from Figure 4. The two parameters n and I_0 nearly have the same behavior as for $T_a=28^\circ\text{C}$ for irradiance intensity $<800 \text{ W/m}^2$ where n decreases from 3.25 to 2.35 and I_0 from about $0.95 \times 10^{-4} \text{ A}$ to about $0.5 \times 10^{-4} \text{ A}$. On the other hand, at high irradiance values ($\geq 800 \text{ W/m}^2$), I_0 and n starts to increase again as previously discussed for $T_a=28^\circ\text{C}$. However, in this case n increases to 2.75 which is lower than the value 3.4 which is achieved for $T_a=28^\circ\text{C}$. Als, I_0 increases to a higher value ($1.5 \times 10^{-4} \text{ A}$) than the value of $1.2 \times 10^{-4} \text{ A}$ which was reached for $T_a=28^\circ\text{C}$. This means that the defect states created at high intensity levels are higher at $T_a=38^\circ\text{C}$.

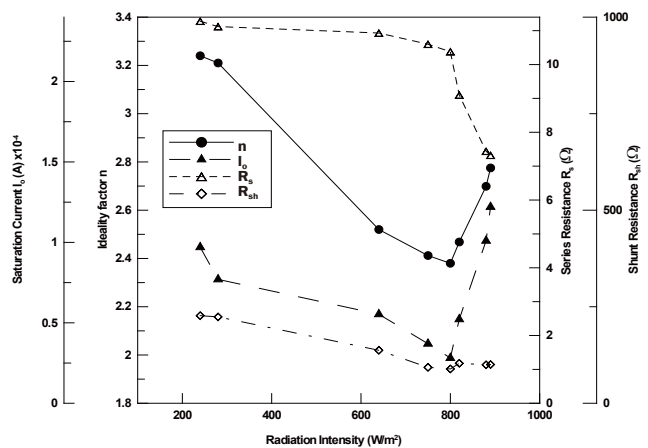


Figure 3
The Module Parameters Variation with Radiation Intensity at Ambient Temperature 38°C

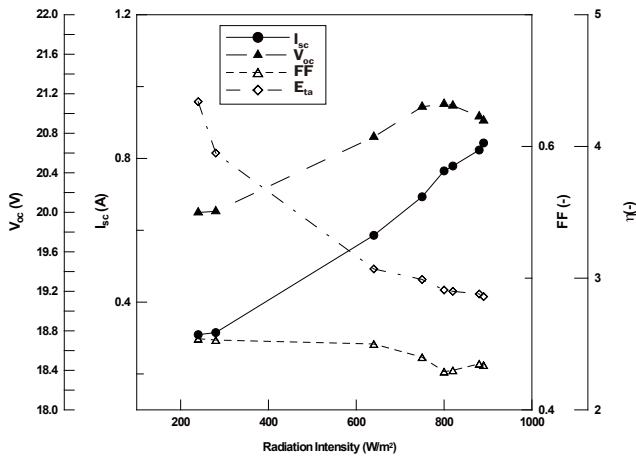


Figure 4
Variation of Module Performance Parameters with Radiation Intensity at Ambient Temperature 38°C

For R_s the first part shown in Figure 4 where R_s increases at first is disappeared at this temperature. This may be due to annealing effects at the contact electrodes. As predicted from the figure, R_s starts to decrease gradually from 11.5Ω to 10.5Ω until irradiance intensity $\leq 800 \text{ W/m}^2$ then R_s starts to decrease dramatically from 10.5 to 7.3Ω this may be attributed to the decrease of the resistance of the pin layers. The behavior of R_{sh} at $T_a=38^\circ\text{C}$ nearly the same as its behavior at lower temperature (28°C) but with a slower rate. The parameter I_{sc} increases linearly from about 0.3 A to about 0.8 A which is higher than the values at $T_a=28^\circ\text{C}$. In this case, V_{oc} behaves oppositely in the whole range of irradiance intensity. As irradiance intensity increases up to 800 W/m^2 , V_{oc} increases from about 20 V to 21.1 V . On the other hand, for irradiance intensity higher than 800 W/m^2 , V_{oc} starts to decrease to 20.9 V . So, the increase in ambient temperature from 28°C to 38°C may causes two effects^[15]:

1st. The band gap of the nip layers particularly the i-layer is effectively decreased resulting in a decrease in V_{oc} and photons with longer wavelengths may be absorbed.

2nd. The minority carrier life time (responsible for photovoltaic effect) can also increase resulting in a slight increase of photo-generated current and thus I_{sc} increases.

At irradiance intensity equal to or lower than 800 W/m^2 , the rate of decrease of n , I_0 and R_s at $T_a=38^\circ\text{C}$ is less than that for $T_a=28^\circ\text{C}$. This behavior produces an overall increase in the V_{oc} and I_{sc} as shown in Figure 4. So, at irradiance intensity $>800 \text{ W/m}^2$, the number of defects increases in the pin layers particularly at the back interface

i/n , causes nearly sharp increase of I_0 and n with sharp decrease of R_s . In this case, the decrease in V_{oc} is bigger than the increase of I_{sc} results in overall decrease of the fill factor and the efficiency as appeared in Figure 4.

Figures 5 and 6 present the variations of module parameters and the corresponding module performance parameters at $T_a=48^\circ\text{C}$. This behavior previously predicted in Figures 3 and 4 is confirmed again in Figures 5 and 6 at the highest ambient temperature studied (48°C). Figure 5 shows that n decreases gradually from about 3.9 to 2.7 without increasing again at higher intensity, which may be due to the stability in the structure inhomogeneity while I_0 decreases gradually with high rate from a value of $5.8 \times 10^{-4} \text{ A}$ to about $(0.8 \times 10^{-4} \text{ A})$ for irradiance intensity $\leq 800 \text{ W/m}^2$ with small increase at irradiance intensity $> 800 \text{ W/m}^2$. On the other hand, R_s increases slightly in the low range of intensity from 11.1 to 11.3Ω then decreases at higher intensity ($\geq 800 \text{ W/m}^2$) to a value of 10.8Ω similar to the behavior predicted at $T_a=28^\circ\text{C}$. So, the performance parameters behavior presented in Figure 6 is similar to the behavior previously obtained in Figure 4 but with lower values of V_{oc} due to temperature effect.

Present results let us conclude that as the ambient temperature increases, the module parameters performance improves as presented in Figure 6. The main improvement occurs in the value of V_{oc} which increases significantly at higher temperatures. This behavior may be attributed to the change in trapping and recombination centers that cause change of space charge distribution which leads to a less distort in the internal electric field across the i-layer. This of course results in an improvement in carrier drift and carrier collection.

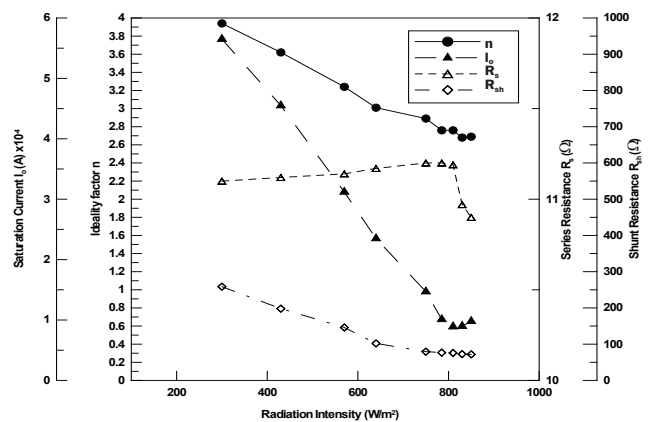


Figure 5
The Module Parameters Variation with Radiation Intensity at Ambient Temperature 48°C

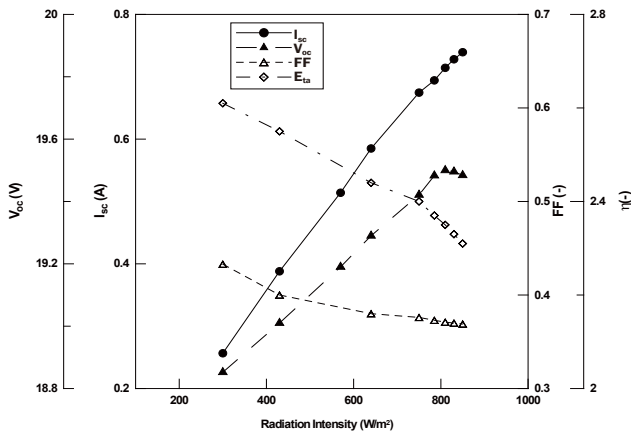


Figure 6
Variation of Module Performance Parameters with Radiation Intensity at Ambient Temperature 48°C

REFERENCES

[1] Poortmans J., & Arkhipov, V. (2006). *Thin Film Solar Cells Fabrication, Characterization and Applications*. John Wiley & Sons Ltd, West Sussex PO19 8SQ, England.

[2] Agarwal S.K., Muralidharan, R., Agarwal, A., Tiwary, V.K., & Jain, S.C. (1981). A New Method for the Measurement of Series Resistance of Solar Cells. *Journal of Physics D: Applied Physics*, 14, 1643-1646.

[3] Chegaar M., Ouennouchi, Z., & Hoffmann, A. (2001). A New Method for Evaluating Illuminated Solar Cell Parameters. *Solid-State Electron*, 45, 293-296.

[4] Ishibashi K.I., Kimura, Y., & Niwano, M. (2008). An Extensively Valid and Stable Method for Derivation of all Parameters of a Solar Cell from a Single Current-Voltage Characteristics. *Journal of Applied Physics*, 103, 094507.

[5] Singh S.N., & Husain, M. (2010). Effect of Illumination Intensity on Cell Parameters of a Silicon Solar Cell. *Solar Energy Materials and Solar Cells*, 94, 1473-1476.

[6] Townsend T.U. (1989). A Method for Estimating the Long-Term Performance of Direct-Coupled Photovoltaic System.

M.Sc. Thesis, Mechanical Engineering, University of Wisconsin-Madison.

[7] Ortiz-Conde A., Garcia Sanchez, F.J., & Muci, J. (2006). New Methods to Extract Model Parameters of Solar Cells from the Explicit Analytic Solutions of Their Illuminated I-V Characteristics. *Solar Energy Materials and Solar Cells*, 90, 352-361.

[8] De Soto W., Klein, S.A., & Beckman, W.A. (2006). Improvement and Validation of a Model for Photovoltaic Array Performance. *Solar Energy*, 80, 78-88.

[9] Burgers A.R. (2004). Fitting Flash Test Curves with ECN's I-V Curve Fitting Program IVFIT. *Proceedings 14th International Photovoltaic Science and Engineering Conference (PVSEC)*. Bangkok, Thailand, 26-30 January.

[10] Klein S.A., et al. (1994). *TRNSYS Users Manual*, Version 14.1. University of Wisconsin Engineering Experimental Station.

[11] Hegedus S.S., & Shafarman, W.S. (2004). Thin-Film Solar Cells: Device Measurements And Analysis. *Progress in Photovoltaics: Research and Applications*, 12(2), 155-176.

[12] Merten J., Asensi, J.M., Voz, C., Shah, A.V., Platz, R., & Andreu, J. (1989). Improved Equivalent Circuit and Analytical Model for Amorphous Silicon Solar Cells and Modules. *IEEE Transaction on Electronic Devices*, 45(2), 423-429.

[13] Radue C., & van Dyk, E.E. (2010). A Comparison of Degradation in Three Amorphous Silicon PV Module Technologies. *Solar Energy Materials and Solar Cells*, 94, 617-622.

[14] Meyer E.L., & van Dyk, E.E., (2004). Assessing the Reliability and Degradation of Photovoltaic Module Performance Parameters. *IEEE Transactions on Reliability*, 53 (1), 83-92.

[15] Del Cueto J.A., & von Roedern, B. (1999). Temperature-Induced Changes in the Performance of Amorphous Silicon Multi-Junction Modules in Controlled Light-Soaking. *Progress in Photovoltaics: Research and Applications*, 7(2), 101-112.